Binary full adder, made of fusion gates, in a subexcitable Belousov-Zhabotinsky system

Andrew Adamatzky[*]
Unconventional Computing Centre, University of the West of England, Bristol, United Kingdom
(Received 22 June 2015; published 28 September 2015)

In an excitable thin-layer Belousov-Zhabotinsky (BZ) medium a localized perturbation leads to the formation of omnidirectional target or spiral waves of excitation. A subexcitable BZ medium responds to asymmetric local perturbation by producing traveling localized excitation wave-fragments, distant relatives of dissipative solitons. The size and life span of an excitation wave-fragment depend on the illumination level of the medium. Under the right conditions the wave-fragments conserve their shape and velocity vectors for extended time periods. I interpret the wave-fragments as values of Boolean variables. When two or more wave-fragments collide they annihilate or merge into a new wave-fragment. States of the logic variables, represented by the wave-fragments, are changed in the result of the collision between the wave-fragments. Thus, a logical gate is implemented. Several theoretical designs and experimental laboratory implementations of Boolean logic gates have been proposed in the past but little has been done cascading the gates into binary arithmetical circuits. I propose a unique design of a binary one-bit full adder based on a fusion gate. A fusion gate is a two-input three-output logical device which calculates the conjunction of the input variables and the conjunction of one input variable with the negation of another input variable. The gate is made of three channels: two channels cross each other at an angle, a third channel starts at the junction. The channels contain a BZ medium. When two excitation wave-fragments, traveling towards each other along input channels, collide at the junction they merge into a single wave-front traveling along the third channel. If there is just one wave-front in the input channel, the front continues its propagation undisturbed. I make a one-bit full adder by cascading two fusion gates. I show how to cascade the adder blocks into a many-bit full adder. I evaluate the feasibility of my designs by simulating the evolution of excitation in the gates and adders using the numerical integration of Oregonator equations.

DOI: 10.1103/PhysRevE.92.032811 PACS number(s): 82.20.Wt, 82.40.Ck

I. INTRODUCTION

Information processing potential of a spatially extended, thin layer, Belousov-Zhabotinsky (BZ) medium [1,2] was first demonstrated in late 1980s in pioneer works by Kuhnert, Agladze, and Krinsky on the experimental laboratory implementation of spatial memory devices and image processing prototypes in the excitable chemical medium [3,4]. Their findings, albeit with a ten-year delay, ignited a series of well-founded theoretical and experimental works on the realization of computing devices in a BZ medium. These include logical gates implemented in geometrically constrained BZ medium [5,6], approximation of shortest path by excitation waves [7–9], memory in BZ micro-emulsion [10], information coding with frequency of oscillations [11], onboard controllers for robots [12–14], chemical diodes [15], BZ neuromorphic architectures [16–19], wave-based counters [20], and other aspects of information processing in excitable chemical systems [21–24].

So far no complete arithmetical circuit has ever been implemented in BZ in experimental conditions. Some preparatory steps have been done. They include simulation and experimental laboratory realization of basic logical gates [25–27,29] and generators of mobile localizations (they can play a role of constant TRUE) in light-sensitive BZ medium [28] and adaptive design of simple logical gates using machine learning techniques [29]. The main reason for such slow experimental progress is the instability of localized excitation wave-fragments: the waves either collapse or expand unless some external periodical stimulation is applied. First a one-bit half-adder in a geometrically constrained light-sensitive BZ medium is proposed in [30], however the implementation required a dynamical update of the illumination level to prevent excitation wave-fragments from collapsing or expanding. Models of a multi-bit binary adder, decoder, and comparator in BZ are proposed in [31–34]. These architectures employ such crossover structures as T-shaped coincidence detectors [35] and chemical diodes [15] that heavily rely on the heterogeneity of geometrically constrained space.

Indeed by controlling excitability [36] in different loci of the medium we can achieve impressive results, as it is demonstrated in works related to polymorphic logical gates [37], analogs of dendritic trees [19], and, particularly, implementation of four-bit input, two-bit output integer square root circuits based on alternating 'conductivity' of junctions between channels [38], however experimental prototypes show a high degree of instability and sensitivity to environmental conditions. In the present paper we try to overcome the problem of excitation wave-fragments instability via combining geometrical-constraining and collision-based approaches.

The paper is structured as follows. We define the Oregonator model of the BZ medium and discuss parameters of simulation in Sec. II. In Sec. III we outline differences in wave-front behavior in an excitable and subexcitable BZ medium. The fusion gate is designed and its behavior is simulated and analyzed in Sec. IV. Section V presents the architecture of a one-bit half-adder made of a fusion gate. Two fusion gates are cascaded into a one-bit full adder in Sec. VI. In Sec. VII we show how to cascade one-bit full adders into a many-bit full adder. Feasibility of the approach is discussed in Sec. VIII.

[*]andrew.adamatzky@uwe.ac.uk

II. MODEL

I use two-variable Oregonator equation [39] adapted to a light-sensitive Belousov-Zhabotinsky (BZ) reaction with applied illumination [40]:

$$\frac{\partial u}{\partial t} = \frac{1}{\epsilon}\left(u - u^2 - (fv + \phi)\frac{u-q}{u+q}\right) + D_u\nabla^2 u,$$
$$\frac{\partial v}{\partial t} = u - v. \qquad (1)$$

The variables u and v represent local concentrations of an activator, or an excitatory component of the BZ system, and an inhibitor, or a refractory component. Parameter ϵ sets up a ratio of the time scale of variables u and v, q is a scaling parameter depending on rates of activation/propagation and inhibition, f is a stoichiometric coefficient. Constant ϕ is a rate of inhibitor production. In a light-sensitive BZ ϕ represents the rate of inhibitor production proportional to intensity of illumination (1).

We integrate the system using Euler method with five-node Laplace operator, time step $\Delta t = 0.001$, and grid point spacing $\Delta x = 0.25$, $\epsilon = 0.02$ (see Sec. III), $f = 1.4$, $q = 0.002$. The parameter ϕ characterizes the excitability of the simulated medium.

To generate excitation waves of wave-fragments I perturb the medium by square solid domains of excitation, 10×10 sites in state $u = 1.0$; if a different shape of perturbation was used we indicate this in the captions of the figures.

The medium is excitable and exhibits 'classical' target waves when $\phi = 0.05$ and the medium is subexcitable with propagating localizations, or wave-fragments, when $\phi = 0.0766$. Time lapse snapshots provided in the paper were recorded at every 150 time steps, I display sites with $u > 0.04$.

The model has been repeatedly verified by me in experimental laboratory studies of the BZ system, and the perfect match between the model and the experiments was demonstrated in [26–29].

I adopt the following symbolic notations: Boolean variables x and y take values '0', logical FALSE, and '1', logical TRUE; xy is a conjunction (operation AND), $x \oplus y$ is exclusive disjunction (operation XOR), $\overline{x}$ is a negation of variable x (NOT). Disjunction (OR) of variables x and y is $x + y$.

III. EXCITABLE VERSUS SUBEXCITABLE MEDIA

Given an initial asymmetric excitation domain a wave-fragment is formed. The fragment's velocity vector is a normal to longest side of the perturbation domain. The medium is excited by rectangular domains of perturbed sites. The perturbation domains are elongated along the north-south axis therefore wave-fragments generated propagate west and east. In the excitable medium, with a low threshold of excitation, every resting site neighboring excited site becomes excited. Therefore literally a point-wise excitation is enough to generate a full-scale omni-directional wave. In a subexcitable medium a resting site needs several excited neighbors to get excited. Initially an asymmetric wave will cause the excitation of resting sites residing near the middle of the wave-front only. Therefore the excitation wave-fragment 'grows' from its center and 'dies' at its ends. This is why wave-fragments in Fig. 1 propagate only east and west and shrink or just slightly expand along the south-north direction.

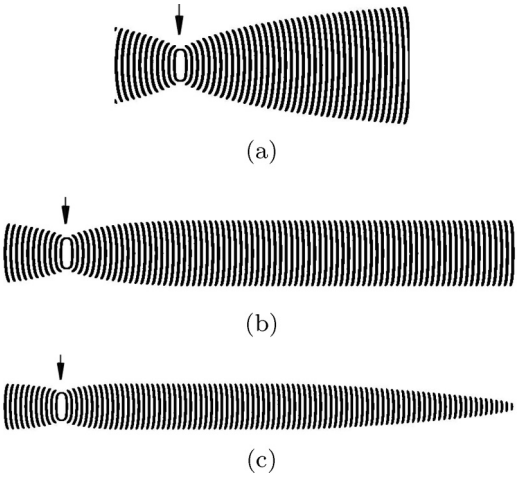

FIG. 1. Time-lapsed snapshots of wave-fragments propagating in simulated BZ medium in (a) near lower threshold of excitability, $\phi = 0.079$, (b) subexcitable mode, $\phi = 0.07905$, (c) non-excitable mode, $\phi = 0.0791$. The media were perturbed by rectangular north-south elongated domains of excitation, 3×40 sites in state $u = 1.0$. Sites of initial segment-wise perturbation are shown by arrows. Grid size is 1125×250 nodes. The pictures are not snapshots of many wave fronts generated at the initial stimulation point. These are time-lapsed snapshots of two waves (one propagating right, another left) recorded every 150th step of numerical integration.

Depending on the medium's excitability wave-fragments may expand [Fig. 1(a)], keep their shape for a long time [Fig. 1(b)], or collapse [Fig. 1(c)]. In an ideal situation, assuming that wave-fragments keep their shapes indefinitely, we can implement a collision-based computing circuit of any depth subject to space availability. However in reality, particularly in conditions of chemical laboratory experiments, wave-fragments are very unstable. It is almost impossible to keep a medium at the precise level of subexcitability [Fig. 1(b)], and almost any wave-fragment will expand [Fig. 1(a)] or collapse [Fig. 1(c)].

It is possible to keep a wave-fragment from collapsing or exploding by periodically changing the excitability of the medium [41]. When a wave-fragment expands we increase the illumination level thus decreasing the medium's excitability. When the wave-fragment starts to collapse the illumination is decreased, the medium's excitability increases and the wave-fragment expands. In designs of logical circuits when channels are represented by shadowed areas and other parts of medium with illuminated areas, it would be difficult to keep the periodicity of illumination and synchronize signals at the same time. Therefore, I adopted the following approach. I keep the medium in excitable mode inside channels and in subexcitable mode at the junctions. Thus I do not worry about the collapsing of wave-fronts inside channels, yet we keep wave-fronts localized when they cross junctions between channels.

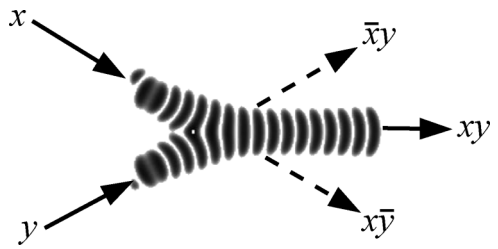

FIG. 2. Time-lapsed overlays of the fusion of two excitation wave-fragments. One fragment is traveling from north-west to south-east, another fragment from south-west to north-east. The wave-fragments collide and fuse into a new localized excitation traveling east.

IV. FUSION GATE

When two wave-fragments, of equal size, traveling towards each other in a subexcitable medium collide head-on, they annihilate. When the wave-fragments collide at an acute angle they fuse into a single wave-fragment (Fig. 2). If one of the wave-fragments was present another fragment would move along its original trajectory.

This gives us an idea of a fusion gate. The gate is built of channels and junctions containing BZ medium. The medium is in excitable mode in the channels, $\phi = 0.05$ in Eq. (1), and the medium is in subexcitable mode in the junctions, $\phi = 0.0766$ in Eq. (1), see the subexcitable domain marked in grey in Fig. 4(g). The gate has two input channels and three outputs channels [Fig. 3(a)]. When there is a wave-fragment present in the input channel x (y) I assume that input variable x (y) takes logical Boolean value TRUE, $x = 1$ ($y = 1$); otherwise the Boolean value FALSE, $x = 0$ ($y = 0$).

If the gate is in excitable mode and initiated with input $x = 1$ and $y = 0$ [Figs. 3(b) and 4(a,b)], then the wave-fragment propagating along input channel x expands at the junction [Fig. 4(c,d)]. Excitation wave-front then enters all other channels [Figs. 3(b) and 4(e,f)]. Such a gate implements only the multiplication of a signal and it is not useful for a realization of logical functions. If the gate is in a subexcitable mode and initiated with $x = 1$ and $y = 0$ [Figs. 3(c) and 4(g,h)] then the wave-fragment does not expand at the junction [Fig. 4(i,j)] but continues through the junction along its original trajectory [Fig. 4(k,l)].

If the gate was in excitable mode and initiated with input $x = 1$ and $y = 1$ [Fig. 3(d)] the wave-fragments collide, fuse, and expand. The excitation wave-fronts enter all three output channels. In subexcitable mode the wave-fragments fuse [Fig. 3(e)] into a single localized wave-fragment which enters the central output channel (Fig. 5).

Thus, assuming that the presence of a wave-fragment in an output channel symbolizes the logical variable in state TRUE at the output channel, we conclude that the fusion gate, being in subexcitable mode, implements a two-input–three-output Boolean logic gate $\langle x, y\rangle \to \langle \bar{x}y, xy, x\bar{y}\rangle$ [Fig. 3(a)]. The fusion gate is a key component of a one-bit half-adder presented in the next section.

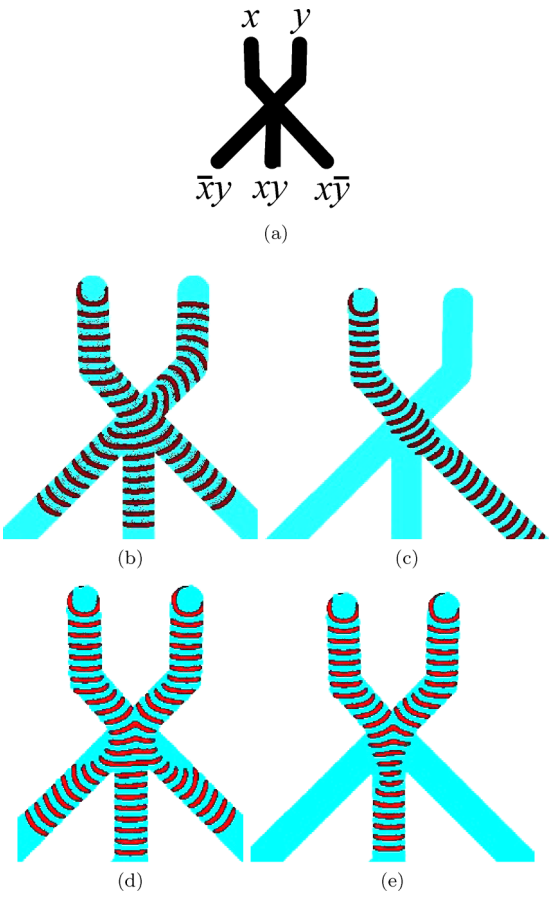

FIG. 3. (Color online) Fusion gate. (a) Scheme: inputs are x and y, outputs are xy, $\bar{x}y$, $x\bar{y}$. (a–d) Time-lapsed overlays of excitation waves. (b) Excitable mode, $x = 1$, $y = 0$. (c) Subexcitable mode, $x = 1$, $y = 0$. (d) Excitable mode, $x = 1$, $y = 1$. (e) Subexcitable mode, $x = 1$, $y = 1$.

V. HALF-ADDER

A one-bit half-adder is a device with two inputs x and y and two outputs xy (Carry out) and $x \oplus y$ (Sum). The half-adder based on the fusion gate is shown in Fig. 6. It consists of two input channels a and b and two output channels g and h. Presence/absence of a wave-fragment in an input/output channel symbolizes logical TRUE/FALSE state of the input variable assigned to the channel. Synchronization of signal wave-fragments is achieved geometrically: $|a| + |e| + |g| = |b| + |d| + |g| = |a| + |f| + |h|$, where $|\cdot|$ is a length of a channel (Fig. 6).

The half-adder has three junctions c, i, and j (Fig. 6). The junction c is a key part of the fusion gate [Fig. 3(a)] and propagation of wave-fragments through this junction has been discussed in Sec. III. Propagation of waves via junctions i and j is illustrated in Fig. 7 for excitable [Fig. 7(a,c)] and subexcitable [Fig. 7(b,d)] modes.

If the system was in excitable mode then a wave-fragment entering junction i via channel f would expand and propagate into channels e (above and below the junction) and h [Fig. 7(a)]. Similarly, the wave-fragment entering junction j from channel d expands and propagates into channels j, e, and h [Fig. 7(a)]. Signals are multiplied and thus, again, the

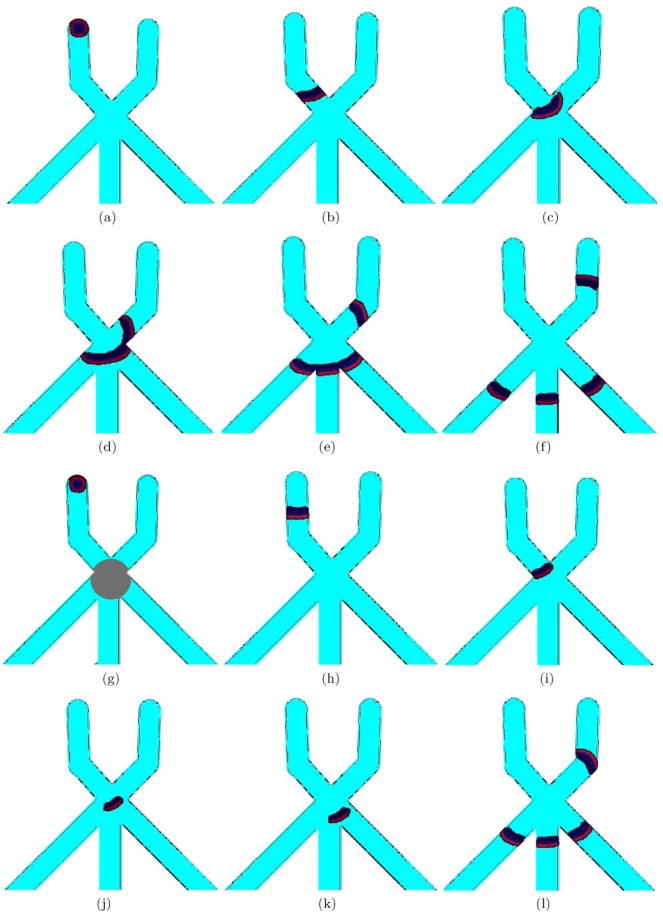

FIG. 4. (Color online) Snapshots of fusion gate for inputs $x = 1$ and $y = 0$. Channels are always in excitable mode, $\phi = 0.05$. (a–f) Junction is in excitable mode [(a) $t = 0.475$, (b) $t = 6.91$, (c) $t = 8.76$, (d) $t = 9.955$, (e) $t = 11.21$, (f) $t = 13.785$]. (g–l) Junction is in subexcitable mode, $\phi = 0.0766$ [(g) $t = 0.37$, (h) $t = 7.14$, (i) $t = 8.785$, (j) $t = 10.135$, (k) $t = 11.31$, (l) $t = 13.605$]. The subexcitable domain is shown in light-gray in snapshot (g). Excitable heads of the wave-fragments are shown in red. Refractory tail in blue.

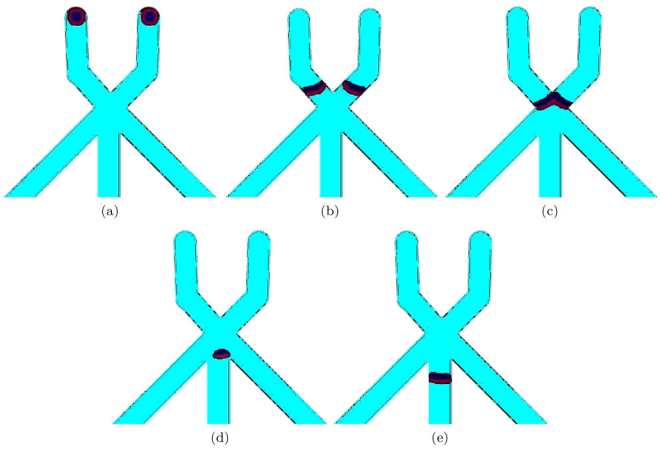

FIG. 5. (Color online) Snapshots of fusion gate for inputs $x = 1$ and $y = 1$. The system is in subexcitable mode. Time is (a) $t = 0.475$, (b) $t = 0.475$, (c) $t = 0.475$, (d) $t = 0.475$, (e) $t = 0.475$. Excitable heads of the wave-fragments are shown in red. Refractory tail in blue.

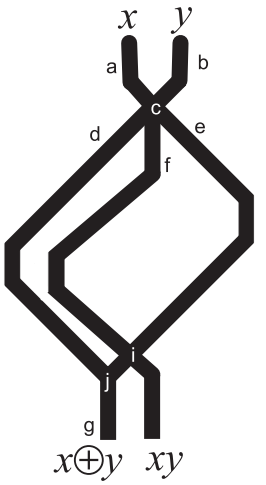

FIG. 6. A scheme of a one-bit half-adder: input channels are a and b, output channels are g and h, internal channels d, e, f, and junctions are c, i, and j. Input variables x and y are fed into channels a and b, results $x \oplus y$ and xy are read from channels g and h.

device being in excitable mode is not useful for implementing logical functions. When the system is in subexcitable mode a wave-fragment entering junction i via channel f stays localized and propagates only into channel h [Fig. 7(b)]. Similarly, a wave-fragment entering junction j from channel d propagates only into channel g [Fig. 7(d)]. There is no such combination of inputs which might lead to a collision of two wave-fragments in junction i, therefore I do not consider such a scenario.

The half-adder in action is shown in Fig. 8. When inputs are $x = 1$ and $y = 0$, a wave-fragment is initiated in channel a. The wave stays localized (without expansion)

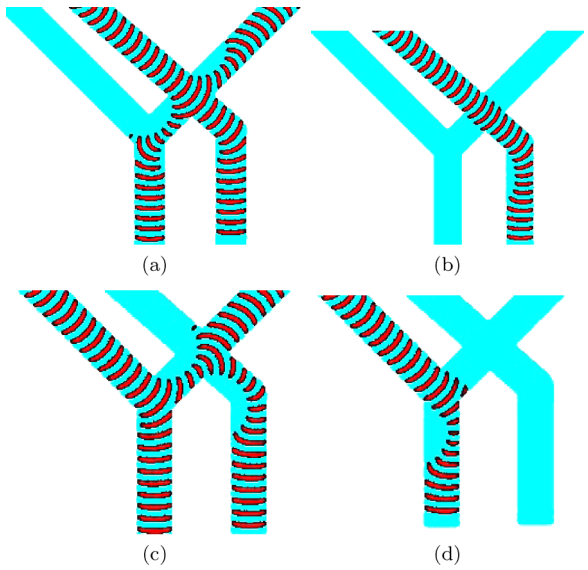

FIG. 7. (Color online) Time lapsed overlays of excitation waves propagating through junctions i (a,b) and j (c,d). (a,b) Wave-fragment approaches junction i via channel f (Fig. 6). (c,d) Wave-fragment approaches junction j via channel d (Fig. 6). (a,c) The system is in excitable mode. (b,d) The system is in subexcitable mode.

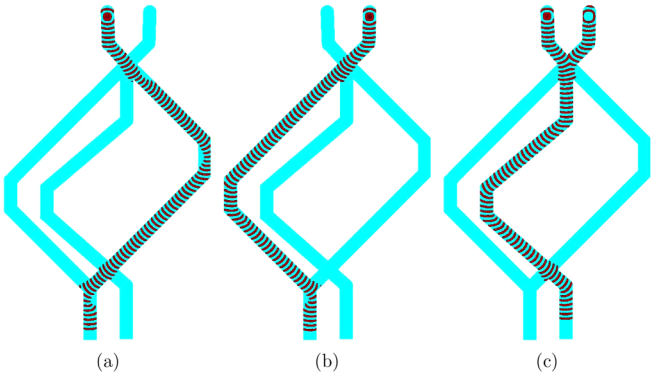

FIG. 8. (Color online) Time lapsed overlays of excitation waves propagation in the one-bit half-adder (Fig. 6) for inputs (a) $x = 1$, $y = 0$, (b) $x = 1$, $y = 0$, (c) $x = 1$, $y = 1$. Sites of initial segment-wise perturbation are visible as discs. Grid size is 500×790 nodes. The pictures are not snapshots of many wave fronts generated at the initial stimulation point. These are time lapsed snapshots of a single wave (a,b) or two waves merging into a single wave (c) recorded every 150th step of numerical integration.

when propagating via junction c and enters channel e. The wave travels along the channel e and through junction i and j and enters output channel g [Fig. 8(a)]. Similarly, when inputs are $x = 0$ and $y = 1$ a wave is initiated in channel b, propagates though junction c, along channel d, via junction j and enters output channel g [Fig. 8(b)]. If both inputs take value TRUE, excitation wave-fragments are initiated in channels a and b simultaneously. The wave-fragments collide at junction c and fuse into a single wave-fragment. This newly born wave-fragment propagates into channel f. The wave travels along channel f, passes though junction i without expansion, and enters the output channel h [Fig. 8(c)].

A wave-fragment appears in output channel g only if a wave-fragment was initiated either in input channel a or input channel b. Therefore, the channel g represents the logical operation $x \oplus y$. A wave-fragment appears in output channel h only if wave-fragments were initiated in input channels x and y. Therefore, the channel h represents logical operation xy. Thus, we illustrated how the half-adder shown in Fig. 6 is derived.

VI. ONE-BIT FULL ADDER

A one-bit full adder is a device with three inputs x, y, and z (Carry in) and two outputs $xy + z(x \oplus y)$ (Carry out) and $x \oplus y \oplus z$ (Sum). The full adder is made of two half-adders (Fig. 9) by cascading Carry in into an input channel of second half-adder, Sum of first half-adder into second input of second half-adder, and Carry out of first half-adder into OR junction with Carry out output channel of second half-adder. The one-bit full adder has three inputs channels a, b, and c (they represent Carry in z, and added bits x and y) and two output channels t and u [they represent sum $x \oplus y \oplus z$ and carry out $xy + z(x \oplus y)$]. Synchronization of signals is achieved geometrically: $|a| + |e| + |p| + |t| = |b| + |h| + |k| + |n| + |t| = |c| + |f| + |k| + |n| + |t| = |b| + |g| + |l| + |u|$. Six junctions d, i, j, m, r, and s are types of junctions already discussed in Sec. VIII.

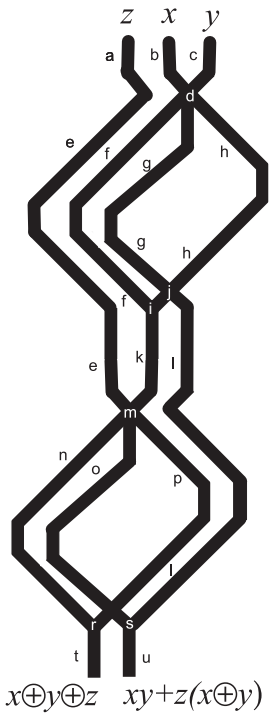

FIG. 9. A scheme of a one-bit full-adder: input channels are a, b, and c, output channels are t and u, internal channels e, f, g, h, k, l, n, o, p, and junctions are d, i, j, m, r, s. Input variables x and y are fed in channels b and c, Carry in is fed in channel a, results $x \oplus y \oplus z$ and $xy + z(x \oplus y)$ are read from channels t and u.

The one-bit full adder in action is shown in Fig. 10. When Carry in has bit up, $z = 1$, and two inputs bits are down, $x = 0$ and $y = z$ the wave-fragment is originated only in input channel a [Fig. 10(a)]. The wave travels along channel

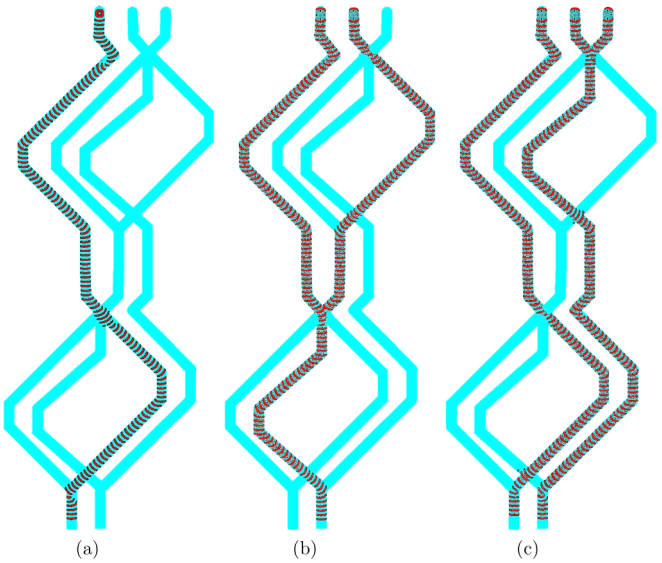

FIG. 10. (Color online) Time lapsed overlays of excitation waves propagation in the one-bit full adder (Fig. 9) for inputs (a) $x = 0$, $y = 0$, $z = 1$; (b) $x = 1$, $y = 0$, $z = 1$; (c) $x = 1$, $y = 1$, $z = 1$.

TABLE I. Schematic dynamic of one-bit full adder for all possible combinations of inputs. The adder, as shown in Fig. 9 is rotated to the left.

x	y	C_{in}	Sum	C_{out}	Configuration
0	0	0	0	0	
1	0	0	1	0	
0	1	0	1	0	
1	1	0	0	1	
0	0	1	1	0	
1	0	1	0	1	
0	1	1	0	1	
1	1	1	1	1	

e, through junction m, enters channel p, propagates though junction r, and finishes its journey in output channel t. For input tuple $z = 0$, $x = 1$, and $y = 0$, an excitation wave-front is initiated in input channel b, propagates through junction d into channel h, through junctions j and i into channel k, through junction n into channel n, and finally enters the output channel t. When inputs are $z = 0$, $x = 0$, and $y = 1$ a wave-front initiated in input channel c propagates through d, along f, through i, along k, through m, along n and ends up in output channel t. For combination of inputs $z = 0$, $x = 1$, and $y = 1$ wave-fragments are initiated in input channels b and c, they merge into a single wave-fragment at junction d. This newly born wave-fragment propagates along g, through j, along l, through s, and into output channel u. Dynamics of excitation waves for inputs $z = 1$, $z = 1$, and $y = 0$ is shown in Fig. 10(b). The wave-fragments merge into a single wave-fragment at junction m and the newly born fragment propagates into output channel u. When all three inputs have a state bit up, $z = 1$, $x = 1$, $y = 1$, the wave-fragment representing $z = 1$ does not interact with the wave-fragment produced by merged wave-fragments representing $x = 1$ and $y = 1$ [Fig. 10(c)]. Thus we have wave-fragments appearing on both output channels t and u.

Trajectories of wave-fragments for all possible combinations of inputs are shown in Table I. The output channel t symbolizes Sum $x \oplus y \oplus z$ and channel u Carry out $xy + z(x \oplus y)$.

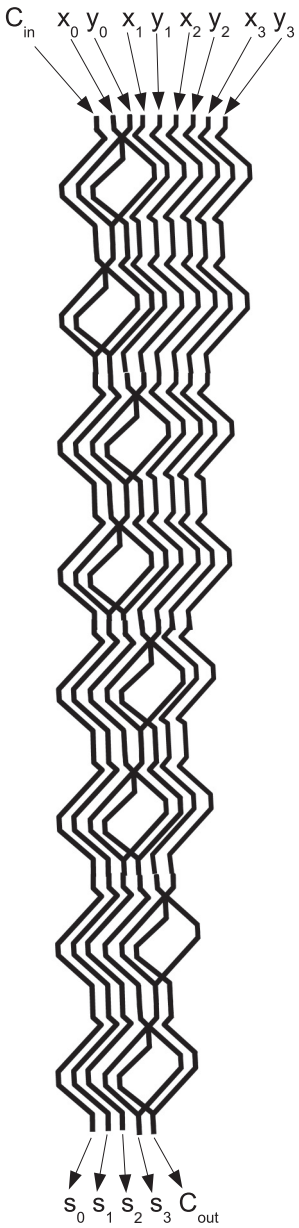

FIG. 11. Scheme of four-bit full adder. Input bit-strings are (x_0,x_1,x_2,x_3) and (y_0,y_1,y_2,y_3) and their sum bit-string is (s_0,s_1,s_2,s_3).

VII. CASCADING ONE-BIT FULL ADDER IN MANY-BITS FULL ADDER

The full adder blocks (Fig. 9) can be straightforwardly cascaded into a many-bit adder. An example of a four-bit adder is shown in Fig. 11. As we can see, an n-bit full adder can be made of $2n$ one-bit half-adders. Signals, represented by wave-fragments, are fully synchronized. Therefore, we can feed input data into the many-bit adder with a period exceeding two wave-widths, so excited heads of current signals do not interfere with refractory tails of previous signals. Assuming that a width of excitation wave-front in a BZ system is circa 0.5–1 mm [42,43], and the speed of propagation is about 1 mm per minute, I believe that many-bits full adder's clock frequency could be 0.01 Hz. With regards to a spatial

complexity, to stay on the safe side I assume that one-bit full adder fits into 10×3 mm box, thus n-bit adder would take $10 \times \ n \times 3$ mm space. That is, e.g., eight-bit adder implemented with fusion gates in subexcitable BZ medium would be 8 cm by 0.3 cm in size.

VIII. DISCUSSION

I proposed the implementation of binary adders in architectures of homogeneous channels in a Belousov-Zhabotinsky (BZ) system. A fusion gate is a key element of the architecture. The function of the fusion gate is to allow lonely excitation wave-fragments to pass along their original trajectories undisturbed but directing a new wave-fragment born after a collision between two wave-fragments along the new trajectory. Localized wave-fragments exist only in a subexcitable BZ system. Unfortunately, they are unstable: after some period of propagation the wave-fragments start expanding or collapsing. Thus to keep the signals propagation without decay, we kept the BZ medium in the excitable mode inside the channel. To prevent signals from exploding at the junction we kept the BZ medium in subexcitable mode at the junctions between the channels. If required, the whole architecture can be kept in subexcitable mode by enforcing periodic changes of excitability.

In experimental laboratory conditions, the architecture can be implemented in two ways. We can make physical templates of the arithmetical circuits, where channels are depressions filled with BZ solution. Such an approach would be robust, however the whole architecture would be non-reconfigurable, and we would still need to apply illumination to control excitability. Using only light would be the most efficient and elegant approach. If BZ medium is light-sensitive then the generation and propagation of waves is controlled by illumination. In the Oregonator model (1) this control is expressed via constant ϕ. This is a rate of inhibitor production proportional to intensity of illumination. Thus the architecture of a computing circuit can be projected onto the medium, in such a manner that channels are black and background is white. Then excitation waves will be confined to the channels because the rest of the medium would be non-excitable. Moreover, by dynamically varying illumination at the junctions we can implement polymorphic logical gates by controlling outcomes of interfragment collisions using the illumination level. For example, in [37] we demonstrated how to switch the BZ collision gate between NOR to XNOR modes.

Let us compare our design with previous implementations (Fig. 12). My previous design of one-bit half-adder implemented in BZ system in computer model [30] and laboratory experiments [44] has four inputs (data signals are duplicated) and four junctions where wave-fragments interact [Fig. 12(a)]. Half-adder implemented in computer models in [33] has two inputs and two outputs and seven junctions, or interactions loci [Fig. 12(b)]. The architecture [33] consists of six disconnected domains of 'conductivity' and has seven junctions, which control propagation of excitation wave-fronts. The half-adder designed in my present paper (Fig. 12(c)) has two inputs and two outputs, only three junctions between channels, and wave-fragments can interact only in two junctions.

Obviously, one can find advantages in every implementation. For example, the first ever BZ half-adder design [30,44] produces a conjunction in addition to Carry out and Sum; and, the design [33] does not require a control of excitability at the junctions. Yet my present architecture seems to be more optimal because it is made of a single domain of 'conductivity' where excitation wave-fragments can interact only in two junctions. Also, speaking in terms of laboratory experiments each coincidence detector [35] and/or chemical diode [15], used in [33], add to the overall unreliability of the system because things can go wrong when excitation waves try to pass loci of discontinuity, because even a width of a channel [45,46] strongly affects the dynamics of wave-fronts.

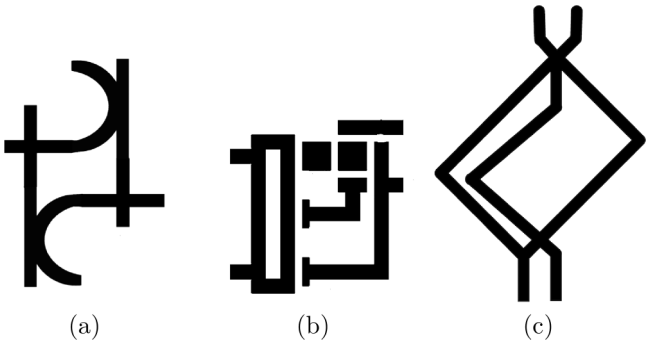

FIG. 12. Architectures of three types of one-bit half-adders implemented in a BZ system. (a) Collision based design [30,44]. (b) Coincidence detectors and chemical diodes based design [33] and (c) wave-fragments fusion based design.

There are three obvious directions of further studies: speed up, application domain, and extension to many-valued circuits. BZ circuits implemented in experimental laboratory conditions are slow, each cycle of computation takes a quarter of an hour. To speed up the computation, I can implement the BZ adders in analog devices [47], molecular arrays [48], and at the nano-scale [49]. With regards to the application domain, I envisage that my designs can be successfully integrated in embedded chemical sensing devices [50,51]. And yet another direction of future research could be in expanding my designs to many-valued logic circuits. In principle, I can implement three-valued gates with wave-fragments in a BZ system [52], based on facilitation or inhibition between two subsequent excitation fronts, more work is required though to achieve cascading of these many-valued logic gates.

And last but not least in my list of 'things-to-do' is an experimental implementation of the fusion gate and adder. In experiments the excitability of the medium will be controlled by the level of illumination. In a BZ medium, reactions are inhibited by high-intensity light. The circuit can be implemented as follows. The whole experimental domain is illuminated with high-intensity. Channels are shadowed, so the medium inside channels is excitable. To make a junction subexcitable I can project solid discs of medium-level illumination onto the junctions. The reviewers reasonably pointed that the circuit might be sensitive to illumination and that it is important to select such a level of junction illumination that the wave-fragment does not 'die' and does not 'explode' while propagating along the junction but keeps its localized shape till it enters the channel. Selecting the right level of illumination might be indeed done by trial and error yet in my previous experimental implementations of competing circuits in a BZ medium [38,44,53] I have shown that the controlling probation of wave-fragments and their

routing by as heterogeneous pattern of illumination is feasible. While doing experimental laboratory implementation I will also address issues of the circuit tolerance to intrinsic noise and possible inhomogeneities in the medium.

ACKNOWLEDGMENT

I thank the reviewers for their constructive comments which helped me to improve quality of the paper a lot.

[1] B. P. Belousov, Compilation of Abstracts on Radiation Medicine **147**, 1 (1959).
[2] A. M. Zhabotinsky, Biofizika **9**, 306 (1964) (in Russian).
[3] L. Kuhnert, Nature **319**, 393 (1986).
[4] L. Kuhnert, K. I. Agladze, and V. I. Krinsky, Nature, **337**, 244 (1989).
[5] O. Steinbock, P. Kettunen, and K. Showalter, J. Phys. Chem. **100**, 18970 (1996).
[6] J. Sielewiesiuk and J. Górecki, J. Phys. Chem. A **105**, 8189 (2001).
[7] O. Steinbock, Á. Tóth, and K. Showalter, Science **267**, 868 (1995).
[8] N. G. Rambidi and D. Yakovenchuk, Phys. Rev. E **63**, 026607 (2001).
[9] A. Adamatzky and B. de Lacy Costello, Naturwissenschaften **89**, 474 (2002).
[10] A. Kaminaga, V. K. Vanag, and I. R. Epstein, Angew. Chem. Int. Ed. **45**, 3087 (2006).
[11] J. Gorecki, J. N. Gorecka, and A. Adamatzky, Phys. Rev. E **89**, 042910 (2014).
[12] A. Adamatzky, B. de Lacy Costello, C. Melhuish, and N. Ratcliffe, Mater. Sci. Eng.: C **24**, 541 (2004).
[13] H. Yokoi, A. Adamatzky, B. de Lacy Costello, and C. Melhuish, Int. J. Bifurcation Chaos **14**, 3347 (2004).
[14] A. Vazquez-Otero, J. Faigl, N. Duro, and R. Dormido, Int. J. Unconv. Comput. **10**, 295 (2014).
[15] Y. Igarashi and J. Gorecki, Int. J. Unconv. Comput. **7**, 141 (2011).
[16] J. Gorecki, J. N. Gorecka, and Y. Igarashi, Nat. Comput. **8**, 473 (2009).
[17] P. L. Gentili, V. Horváth, V. K. Vanag, and I. R. Epstein, Int. J. Unconv. Comput. **2**, 177 (2012).
[18] J. H. Stovold and S. O'Keefe, Simulating neurons in reaction-diffusion chemistry, in *9th International Conference on Information Processing in Cells and Tissues (IPCAT)*, Lecture Notes in Computer Science Vol. 7223 (Springer, Berlin, 2012), pp. 143–149.
[19] H. Takigawa-Imamura and I. N. Motoike, Neural Networks **24**, 1143 (2011).
[20] J. Gorecki, K. Yoshikawa, and Y. Igarashi, J. Phys. Chem. A **107**, 1664 (2003).
[21] K. Yoshikawa, I. N. Motoike, T. Ichino, T. Yamaguchi, Y. Igarashi, J. Górecki, and J. N. Górecka, Int. J. Unconv. Comput. **5**, 3 (2009).
[22] G. Escuela, G. Gruenert, and P. Dittrich, Nat. Comput. **13**, 247 (2014).
[23] G. Gruenert, K. Gizynski, G. Escuela, B. Ibrahim, J. Gorecki, and P. Dittrich, Int. J. Neural Syst. **25**, 1450032 (2014).
[24] J. Gorecki, K. Gizynski, J. Guzowski, J. Gorecka, P. Garstecki, G. Gruenert, and P. Dittrich, Phil. Trans. R. Soc. A **373**, 20140219 (2015).
[25] A. Adamatzky, Chaos, Solitons & Fractals **21**, 1259 (2004).
[26] A. Adamatzky and B. de Lacy Costello, Chaos, Solitons & Fractals **34**, 307 (2007).
[27] A. Adamatzky, B. De Lacy Costello, L. Bull, and J. Holley, Isr. J. Chem. **51**, 56 (2011).
[28] B. de Lacy Costello, R. Toth, C. Stone, A. Adamatzky, and L. Bull, Phys. Rev. E **79**, 026114 (2009).
[29] R. Toth, C. Stone, A. Adamatzky, B. de Lacy Costello, and L. Bull, Chaos, Solitons & Fractals **41**, 1605 (2009).
[30] A. Adamatzky, arXiv:1005.2301.
[31] M.-Z. Sun and X. Zhao, J. Chem. Phys. **138**, 114106 (2013).
[32] G.-M. Zhang, I. Wong, M.-T. Chou, and X. Zhao, J. Chem. Phys. **136**, 164108 (2012).
[33] M.-Z. Sun and X. Zhao, Int. J. Unconv. Comput. **11**, 165 (2015).
[34] S. Guo, M.-Z. Sun, and X. Han, Int. J. Unconv. Comput. **11**, 131 (2015).
[35] J. Gorecka and J. Gorecki, Phys. Rev. E **67**, 067203 (2003).
[36] Y. Igarashi, J. Gorecki, and J. N. Gorecka, *Unconventional Computation* (Springer, Berlin, 2006), pp. 130–138.
[37] A. Adamatzky, B. de Lacy Costello, and L. Bull, Int. J. Bifurcation Chaos **21**, 1977 (2011).
[38] W. M. Stevens, A. Adamatzky, I. Jahan, and B. de Lacy Costello, Phys. Rev. E **85**, 066129 (2012).
[39] R. J. Field and R. M. Noyes, J. Chem. Phys. **60**, 1877 (1974).
[40] V. Beato and H. Engel, *SPIE's First International Symposium on Fluctuations and Noise* (International Society for Optics and Photonics, Bellingham, Washington, USA, 2003), pp. 353–362.
[41] T. Sakurai, E. Mihaliuk, F. Chirila, and K. Showalter, Science **296**, 2009 (2002).
[42] B. T. Ginn, B. Steinbock, M. Kahveci, and O. Steinbock, J. Phys. Chem. A **108**, 1325 (2004).
[43] V. Davydov, N. Manz, O. Steinbock, and S. Müller, EPL (Europhys. Lett.) **59**, 344 (2002).
[44] B. D. L. Costello, A. Adamatzky, I. Jahan, and L. Zhang, Chem. Phys. **381**, 88 (2011).
[45] J. Szymanski and J. Gorecki, Int. J. Unconv. Comput. **6**, 461 (2010).
[46] H. Kitahata, R. Aihara, Y. Mori, and K. Yoshikawa, J. Phys. Chem. B **108**, 18956 (2004).
[47] T. Asai, Y. Kanazawa, T. Hirose, and Y. Amemiya, Int. J. Unconv. Comput. **1**, 123 (2005).
[48] J. H. Reif, Int. J. Unconv. Comput. **8**, 459 (2012).
[49] Z. Konkoli and G. Wendin, Int. J. Unconv. Comput. **10**, 405 (2014).
[50] S. Nakata, S. Izuhara, K. Masui, and M. R. Islam, Int. J. Unconv. Comput. **5**, 39 (2009).
[51] K. Yoshikawa, H. Nagahara, T. Ichino, J. Gorecki, J. N. Gorecka, and Y. Igarashi, Int. J. Unconv. Comput. **5**, 53 (2009).
[52] I. N. Motoike and A. Adamatzky, Chaos, Solitons & Fractals **24**, 107 (2005).
[53] J. Holley, I. Jahan, B. De Lacy Costello, L. Bull, and A. Adamatzky, Phys. Rev. E **84**, 056110 (2011).